Journal of Functional Foods 108 (2023) 105721

Contents lists available at ScienceDirect

Journal of Functional Foods

journal homepage: www.elsevier.com/locate/jff

Allulose enhances epithelial barrier function by tight junction regulation via the TLR4/MyD88/NF-κB immune signaling pathway in an intestinal Caco-2 cell model

Jihye Baek [a,1], Jong-Hwa Kim [a,1], YoHan Nam [a], Go-Eun Kim [b], Kyungheon Ryu [b], Soonok Sa [b], Jung-Sook Han [b], Wonyong Kim [a,*]

[a] Department of Microbiology, Chung-Ang University College of Medicine, Seoul 06974, Republic of Korea
[b] Food R&D Center, Samyang Corp, Seongnam 13488, Republic of Korea

ARTICLE INFO

Keywords:
D-allulose
TLR4/MyD88/NF-κB signaling
Tight junction
Immune regulation

ABSTRACT

D-allulose, a fructose isomer with almost zero calories, has been widely used as a food ingredient that is generally recognized as safe. In recent studies, D-allulose has been shown to alleviate some diseases via restoration of the intestinal barrier. To better understand the role of D-allulose in intestinal epithelial barrier function, we conducted experiments to demonstrate its effects. Our results demonstrated that D-allulose increased transepithelial electrical resistance and decreased intestinal barrier function–associated permeability toward 4 kDa FITC–dextran flux in the damaged intestinal epithelial barrier. It also repaired the disruption pattern of tight junction proteins (ZO-1, occludin, and claudin-1) and inhibited the inflammatory response by inhibiting the TLR4/MyD88/NF-κB pathway. Overall, these findings suggest that D-allulose has the potential to be a beneficial food supplement for improving intestinal epithelial barrier dysfunction.

1. Introduction

The intestinal epithelial barrier plays an important role in regulating the permeation of harmful substances (Catalioto, Maggi, & Giuliani, 2011). Normal barrier integrity depends on cell–cell junction complexes, and tight junctions (TJs) are essential for maintaining structure and permeability. TJs are transmembrane proteins include occludin, claudin, junctional adhesion molecule (JAM), and tricelluin, which are linked to the actin cytoskeleton (Chelakkot, Ghim, & Ryu, 2018). Many studies have shown that intestinal barrier dysfunction, known as leaky gut, allows the infiltration of harmful substances from the gut and external pathogens, leading to an uncontrollable immune response, various diseases (such as inflammatory bowel disease), and food allergies (Anderson & Van Itallie, 1995; He et al., 2019; Lee, 2015; Ma, 1997; Ouyang et al., 2022). Therefore, enhancing intestinal integrity and maintaining the intestinal barrier is important.

TJs can be damaged by bacterial-derived lipopolysaccharides (LPS), which are the major outer membrane component of Gram-negative bacteria. Numerous studies have indicated that LPS increases TJ permeability and disrupts intestinal epithelial barrier function through increased toll-like receptor 4 (TLR4) and mediated pro-inflammatory cytokines (Chen et al., 2020; He et al., 2019). Thus, the LPS-induced intestinal damage model is widely used in studies investigating intestinal epithelial barrier dysfunction. In this study, LPS-induced Caco-2 cell monolayers were used to simulate injury to human intestinal epithelial cells and investigate the hypothesis that D-allulose improves intestinal barrier function and changes the expression level of TJ proteins.

Recently, it has been indicated that toll-like receptor 4 (TLR4)–stimulated inflammation in intestinal epithelial cells induces two major signaling pathways: the myeloid differentiation primary response 88 (MyD88)–dependent and TIR-domain-containing adapter-inducing interferon-β (TRIF)–dependent pathways (Kawai & Akira, 2006). In the MyD88-dependent pathway, TLR4 is responsible for binding to MyD88, which connects interleukin-1 receptor–associated kinase (IRAK) and TRAF6 complexes (Tam, Coller, Hughes, Prestidge, & Bowen, 2021). The TLR4 signaling pathway has been associated with intestinal barrier integrity regulation and the inflammatory response (Ciesielska, Matyjek, & Kwiatkowska, 2021; Dheer et al., 2016). Moreover, in the TLR4/NF-

* Corresponding author at: Department of Microbiology, Chung-Ang University College of Medicine, 84, Heukseok-ro, Dongjak-gu, Seoul 06974, South Korea.
E-mail address: kimwy@cau.ac.kr (W. Kim).
[1] These authors contributed equally to this work.

https://doi.org/10.1016/j.jff.2023.105721
Received 18 February 2023; Received in revised form 18 July 2023; Accepted 5 August 2023
Available online 11 August 2023

κB pathway, NF-κB plays a key role in responses to intestinal barrier damage and mucosal immune responses (Luo, Guo, & Zhou, 2012). Furthermore, studies suggest that increased TJ permeability is mediated by downregulation of the TLR4/MyD88/NF-κB signaling pathway (Hasegawa, Mizugaki, Inoue, Kato, & Murakami, 2021; He et al., 2019).

D-allulose (also named D-psicose), a C-3 epimer of D-fructose, is not naturally abundant, but it exists in nature, including in vegetables and fruits. It accounts for 70 % of the sweetness of sucrose and has a similar function to sucrose in the reconstitution of food, with a metabolizable energy value of almost zero calories (Hossain et al., 2015; Matsuo, Suzuki, Hashiguchi, & Izumori, 2002). D-allulose is widely used as a food ingredient that is generally recognized as safe by the U.S. Food and Drug Administration and several countries (FDA, 2012; Franchi et al., 2021). A recent study showed that D-allulose could improve gut mucosal barrier function (Suzuki et al., 2022). D-allulose is also known to affect obesity and type 2 diabetes (Gou et al., 2021; Niibo et al., 2022). However, it is unclear what role allulose plays in the intestinal epithelial barrier function or the regulation of inflammatory responses. Collectively, this study aimed to determine the effects of D-allulose on intestinal permeability and to determine its underlying molecular mechanisms in the LPS-induced Caco-2 cell model of inflammation-mediated barrier dysfunction.

2. Material and methods

2.1. Reagents and materials

D-allulose powder (purity, >98 %) was obtained from Samyang Corporation, Republic of Korea. LPS (O111:B4; L2630), 3-(4,5-dimethylthiazol-2-yl)-2,5-diphenyltetrazolium bromide (MTT), radioimmunoprecipitation (RIPA) lysis buffer, TRIzol reagent, bovine serum albumin (BSA), 2′7′-dichlorofluorescein-diacetate (DCFH-DA), fluorescein isothiocyanate–dextran 4000 (FD-4; molecular weight, 4 kDa), dimethyl sulfoxide (DMSO), and 4′,6-diamidino-2-phenylindole (DAPI) were purchased from Sigma-Aldrich (St. Louis, MO, USA). Hanks buffer solution, fetal bovine serum (FBS), Dulbecco's modified Eagle medium (DMEM), and penicillin/streptomycin were obtained from Gibco (BRL, Grand Island, NY, USA). Protease inhibitor (#78425) and PicoEPD reagent (EBP-1073) were purchased from Thermo Fisher Scientific (Waltham, MA, USA). Primary antibodies against ZO-1 (#8193), occludin (#91131), claudin-1 (#13995), p65 (#4842), phospho-p65 (#3033), MyD88 (#3699), IKKα (#2682), IKKβ (#8943), phospho-IKKα/β (#2697), IκBα (#4812), phospho-IκBα (#2859), and glyceraldehyde 3-phosphate dehydrogenase (GAPDH, #5174), as well as horseradish peroxidase (HRP) goat anti-rabbit IgG (#2895), were purchased from Cell Signaling Technology (Danvers, MA, USA). The Prostaglandin E2 Human ELISA kit was obtained from R&D Systems (Minneapolis, MN, USA).

2.2. Cell culture and treatment

Human intestinal Caco-2 cells were maintained routinely in 25-cm^2 cell culture flasks at 37 °C in a 5 % CO_2 incubator. Caco-2 cells were grown in DMEM medium supplemented with 10 % FBS. The culture medium was refreshed every 2 days during cell growth and differentiation. For the experiments, cells were used 14–21 days after reaching the confluence point for differentiation into epithelial cells. Caco-2 cells used in all experiments had gone through 10–25 passages. D-allulose was dissolved and diluted to the desired concentrations with the basic medium. The cells were subjected to treatments with three different D-allulose concentrations for 24 h: 5, 10, and 20 mM. For the transepithelial electrical resistance (TEER) and permeability experiments, Caco-2 cells (density, 5×10^4 cells) were inoculated into the chambers of Transwell inserts (Millicell Cell Culture Insert, 12 mm, polycarbonate, 0.4 μm) in 24-well plates (Corning, USA) and cultured for 21 days to induce differentiation. The Caco-2 cells were ready for experiments when the TEER reached 200 Ω·cm^2. For the quantitative real-time polymerase chain reaction (qRT-PCR), Western blot, and reactive oxygen species (ROS) experiments, cells (density, 2×10^5/well) were cultured in 24-well plates.

2.3. Cell viability assay

Viability was assessed in Caco-2 cells. Cells were seeded in 96-well culture plates (5×10^4 cells/well) and incubated for 24 h. Cells were washed twice in PBS and then cultured in a serum-free medium for 12 h. The monolayers were coincubated with LPS (1 μg/mL) in the presence or absence of D-allulose (5, 10, and 20 mM) and incubated for 24 h. Thereafter, MTT solution (0.5 mg/mL) was added for 2 h. The absorbance of the MTT-formazan product was read using an Infinite 200 NanoQuant microplate reader (Tecan, Männedorf, Switzerland) at 590 nm after being dissolved with 200 μL/well DMSO.

2.4. Measurement of intracellular ROS production

The ROS assay involved measuring the fluorescence flux of DCFH-DA in LPS-induced Caco-2 cells, as described elsewhere (Wolfe & Liu, 2007). In brief, after the culture medium was removed, DCFH-DA (20 μM) was added to the cells and incubated for 30 min at 37 °C. Then the cells were washed three times with PBS. Cells were observed using a microplate reader (Tecan) with excitation at 488 nm and emission at 535 nm. Three biological replicates were performed for each experiment, and the results were calculated as the percentage of control cells.

2.5. TEER measurements

TEER, which can reflect TJ permeability to ionic solutes, was assessed as per a previously described method (Li et al., 2019). Briefly, Caco-2 cells (5×10^4 cells/mL) were inoculated on Transwell inserts of 24-well plates before aliquots (600 μL) of culture medium were placed in the basolateral compartment. The cells were ready for experiments when the transepithelial electrical resistance (TEER) reached 200 Ω ^{cm2}. TEER values were measured using a Millicell-ERS-2 V-ohmmeter (Millipore, Bedford, MA, USA). The three wells around the cell were measured repeatedly until the same result was recorded three times. The values were taken as the measured electrical resistance through the mean of the three holes and calculated in Ω·cm^2.

2.6. Paracellular permeability assay

To assess paracellular permeability of Caco-2 cell monolayers was determined as previously described (Lan, Zhang, He, Li, Zeng, Qian, & Song, 2021). Briefly, to determine the influx rate of FD-4 across Caco-2 monolayers, 200 μL of FD-4 (100 μg/mL) solution was added into the apical chamber, while aliquots (600 μL) of Hanks buffer solution were added to the basolateral side. Then, after the cells were incubated for 2 h, samples were withdrawn from the basolateral side, which was quantified using a microplate reader (Tecan) with excitation at 485 nm and emission at 535 nm. Three biological replicates were performed for each experiment.

2.7. Determination of prostaglandin E_2

Caco-2 cells (2×10^5 cells/mL) were incubated for 24 h with D-allulose (5, 10, and 20 mM) and LPS (1 μg/mL) in a complete medium. The cells were centrifuged at 1000 g for 5 min, and prostaglandin E_2 (PGE_2) levels were determined in the supernatant using a monoclonal enzyme-linked immunosorbent assay (ELISA) kit (R&D Systems) according to the manufacturer's instructions. Absorbance was read at 405 nm using a microplate reader.

2.8. Total RNA extraction and qRT-PCR

Total RNA was extracted using TRIzol reagent, and the cDNA was synthesized using the Primescript first-strand cDNA synthesis kit (Takara Bio, Shiga, Japan). The qRT-PCR was performed using a Quant3 real-time PCR system (Applied Biosystems, Foster City, CA, USA) with an SYBR Green Master Mix. The levels of gene expression were quantified using the $2^{-\Delta\Delta Ct}$ method, and the GAPDH gene was used as the reference gene. The primer sequences are listed in Table S1.

2.9. Western blot assay

For the protein expression analysis, total protein from Caco-2 cells was extracted using RIPA lysis buffer containing protease inhibitors. The protein was assessed with a bicinchoninic acid protein assay kit (Abcam, Cambridge, UK). The appropriate amount of protein was separated by 10 % sodium dodecyl sulfate–polyacrylamide gel electrophoresis, transferred to PVDF membranes (Hercules, CA, USA), and then blocked with 5 % BSA for 1 h at room temperature. The membranes were incubated with primary antibodies overnight at 4 °C and then incubated with secondary antibodies conjugated with HRP for 1 h. Blots were washed with Tris-buffered saline and Tween 20 and then developed with PicoEPD Western blot detection reagents. The protein intensity was quantified using ImageJ, version 1.5.3 (National Institutes of Health, Bethesda, MD, USA).

2.10. Immunofluorescent localization of TJ proteins

Caco-2 monolayers were cultured for 21 days and treated with D-allulose (5, 10, and 20 mM) and LPS (1 μg/mL) for 24 h. For immunofluorescent localization of the TJ proteins, cells were fixed with 4 % formaldehyde for 15 min at 37 °C and then infiltrated with Triton X-100 for 30 min at room temperature. Then, the cells were blocked with 2 % BSA in PBS for 1 h and incubated overnight at 4 °C with primary antibodies against ZO-1 (1:200) or occludin (1:500) and claudin-1 (1:200). Cells were then probed using the secondary antibodies—goat anti-rabbit Alexa 488 or goat anti-mouse Alexa 647 at room temperature for 1 h. Nuclei were stained using DAPI solution of concentration 1 μg/mL for 5 min at room temperature. Co-localization images were obtained using a microscope (Olympus Opticals, Tokyo, Japan).

2.11. Statistical analysis

All experiments were carried out in triplicate, and the results are expressed as mean ± standard error of the mean (SEM). GraphPad Prism 9.0 (San Diego, CA, USA) was used for statistical analyses. Statistical analysis was performed by one-way analysis of variance (ANOVA) followed by Dunnett's post hoc test for group comparison; $p < 0.05$ was considered statistically significant.

3. Results

3.1. Effect of D-allulose on cell viability

Previous studies have demonstrated that D-allulose (Fig. 1A) exerts beneficial outcomes against anti-adiposity (Lee et al., 2021), reduces postprandial hyperglycemia (Hayashi et al., 2010), and has antioxidant activities (Chung, Oh, & Lee, 2012). The present study aimed to explore the effects of D-allulose on Caco-2 cell viability after LPS or without LPS (Fig. 1B–C). Varying concentrations of D-allulose (5, 10, and 20 mM) with LPS or without LPS for 24 h clearly had no toxic effects on Caco-2 cell viability. We then determined whether non-toxic D-allulose concentrations protected Caco-2 cells against LPS-induced cytotoxicity by analyzing intracellular ROS levels. D-allulose treatment significantly decreased the ROS levels relative to the LPS group (Fig. 1D). Based on these results, 5, 10, and 20 mM D-allulose were used for the subsequent experiments.

3.2. Effect of D-allulose on TEER and paracellular permeability

The TEER of the Caco-2 cell monolayers was significantly decreased after treatment with TNF-α, and this decrease was significantly alleviated by D-allulose (5, 10, and 20 mM) ($P < 0.0001$) (Fig. 2A). In accordance with the TEER values, the paracellular dextran flux of FD-4

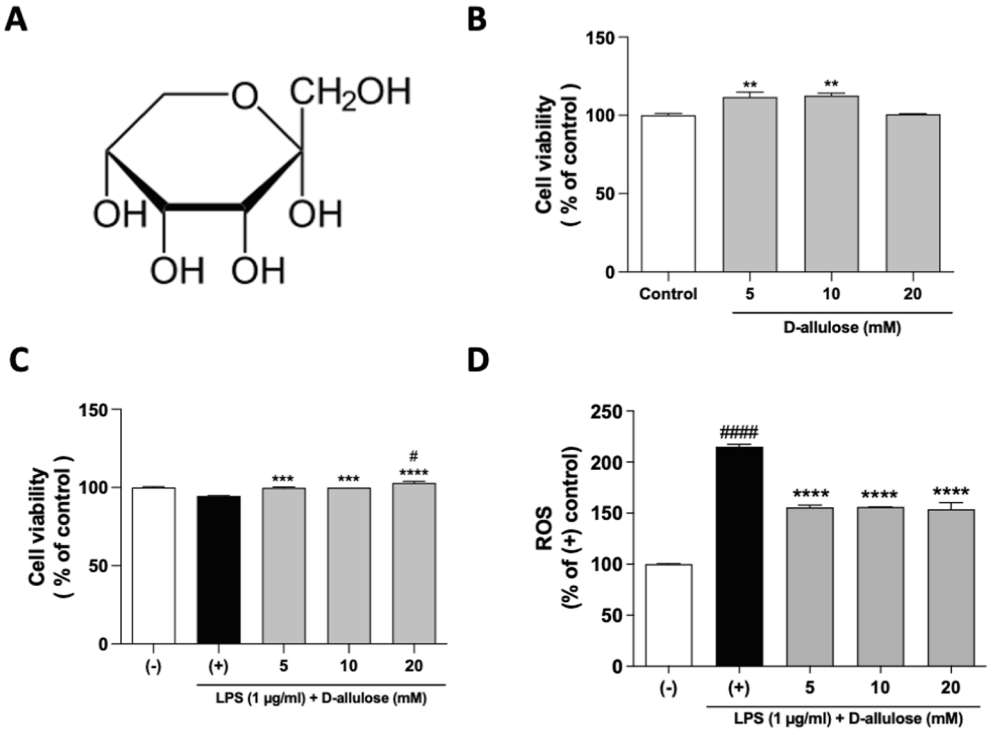

Fig. 1. Cytotoxicity of D-allulose and cytoprotective effect through inhibition of ROS in LPS-induced Caco-2 cells. (A) Cytotoxicity to dose response of D-allulose was evaluated using the MTT assay. (B) The dose–effect of D-allulose was evaluated by measuring LPS-induced ROS production in Caco-2 cells. Values are expressed as percentage of control group. Results are shown as mean ± standard deviation ($n = 5$). * $p < 0.05$ and **** $p < 0.0001$ versus LPS-treated group. #### $p < 0.0001$ *vs.* control group.

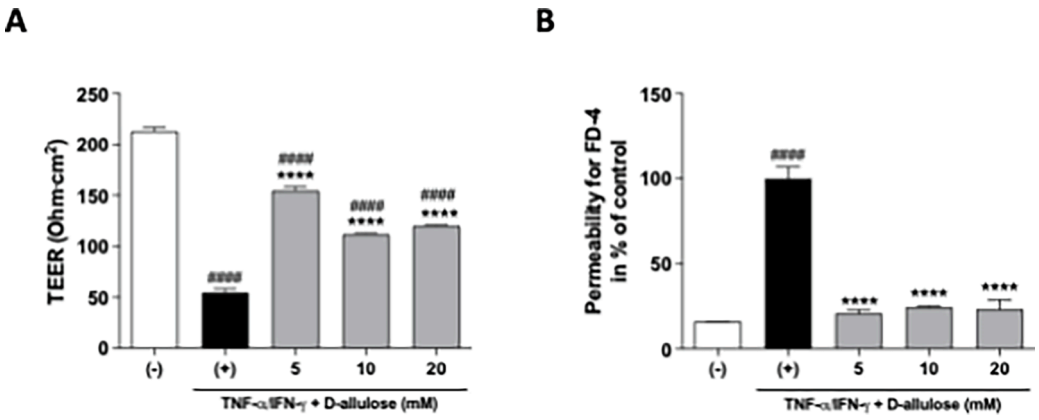

Fig. 2. Effects of D-allulose on epithelial permeability toward 4-kDa FITC-dextran. (A) TEER and (B) FITC-dextran fluorescence was performed on LPS-induced Caco-2 cells. Values are expressed as percentage of TNF-α/IFN-γ group. Results are shown as mean ± standard deviation ($n = 5$). * $P < 0.05$ and **** $P < 0.0001$ *vs.* LPS-treated group. #### $P < 0.0001$ *vs.* control group.

was measured from the apical to the basal direction. As shown in Fig. 2B, the paracellular dextran flux increased in the TNF-α/IFN-γ group, while this effect could be inhibited by D-allulose treatment ($P < 0.05$). According to the results, all concentrations of D-allulose could protect the integrity of Caco-2 cell monolayers from the impairment induced by IFN-γ and TNF-α.

3.3. Effect of D-allulose on pro-inflammatory responses in intestinal epithelial cells

The mRNA levels of TLR4, NF-κB p65, COX-2, IL-1β, TNF-α, and IL-8 were analyzed by qRT-PCR. After stimulation with LPS, the mRNA expression of TLR4, NF-κB p65, COX-2, IL-1β, TNF-α, and IL-8 were significantly increased in the Caco-2 cell monolayers ($P < 0.005$; Fig. 3A–E). D-allulose treatment (10 and 20 mM) dose-dependently decreased the levels of all cytokines compared with those in the LPS group ($P < 0.05$). Furthermore, D-allulose treatment downregulated the expression level of PGE2 ($P < 0.0001$; Fig. 3F).

3.4. Effect of D-allulose on barrier properties and expression in LPS-induced intestinal epithelial barrier dysfunction

The qRT-PCR analysis indicated that LPS treatment significantly decreased the mRNA levels of ZO-1 and occludin in Caco-2 cells (Fig. 4A and 4B). However, D-allulose treatment increased the mRNA levels of ZO-1 and occludin in LPS-treated Caco-2 cell monolayers. At concentrations of 10 and 20 mM, D-allulose significantly increased the mRNA expression of these TJ proteins ($P < 0.001$).

As shown by the Western blot results, the expression of the ZO-1 and occludin proteins was significantly decreased by LPS. However, D-allulose treatment significantly inhibited the downregulation of these TJ proteins ($P < 0.0001$; Fig. 4A and 4B).

3.5. Effects of D-allulose on ZO-1, occludin, and claudin-1 localization and distribution in LPS-induced Caco-2 cells

As shown in Fig. 5, ZO-1 and occludin were appropriately localized to their respective intercellular distributions and were connected without damage in the control group. However, the LPS-treated cells had discontinuous and abnormal structural staining. D-allulose (5, 10,

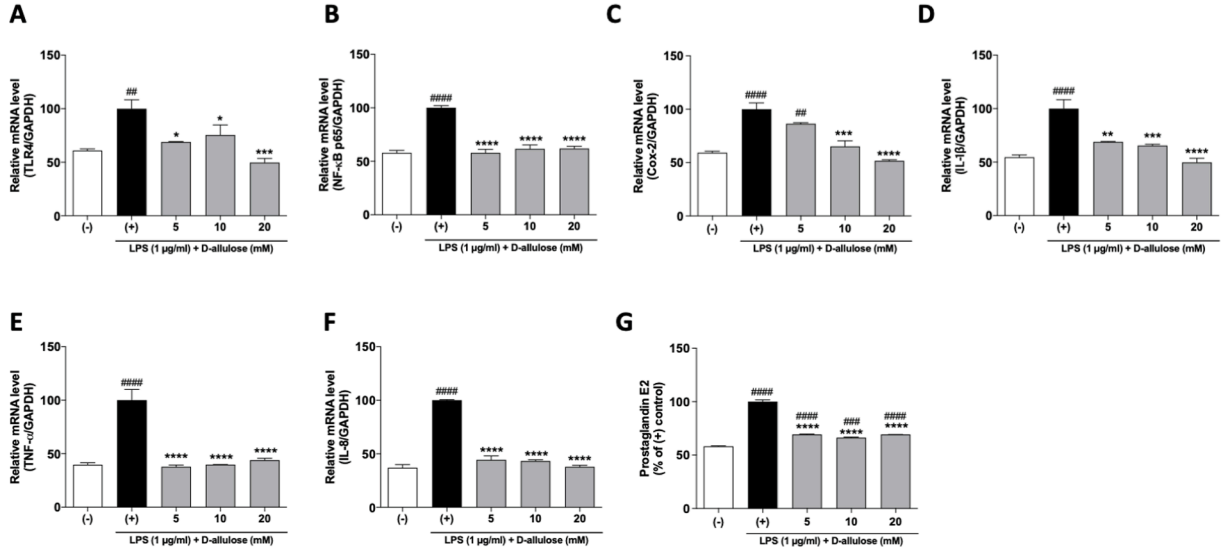

Fig. 3. Effects of D-allulose on inflammatory responses in LPS-induced Caco-2 cells. The mRNA expression levels of (A) TLR4, (B) NF-κB p65, (C) COX-2, (D) IL-1β, (E) TNF-α, and (F) IL-8 were measured using qRT-PCR. (G) PGE_2 was measured using a monoclonal enzyme immunoassay (ELISA). Values are expressed as percentage of the LPS group. Results are shown as mean ± standard deviation ($n = 5$). * $P < 0.05$, ** $P < 0.01$, *** $P < 0.001$ and **** $P < 0.0001$ *vs.* LPS-treated group. ## $p < 0.01$ and #### $P < 0.0001$ *vs.* control group.

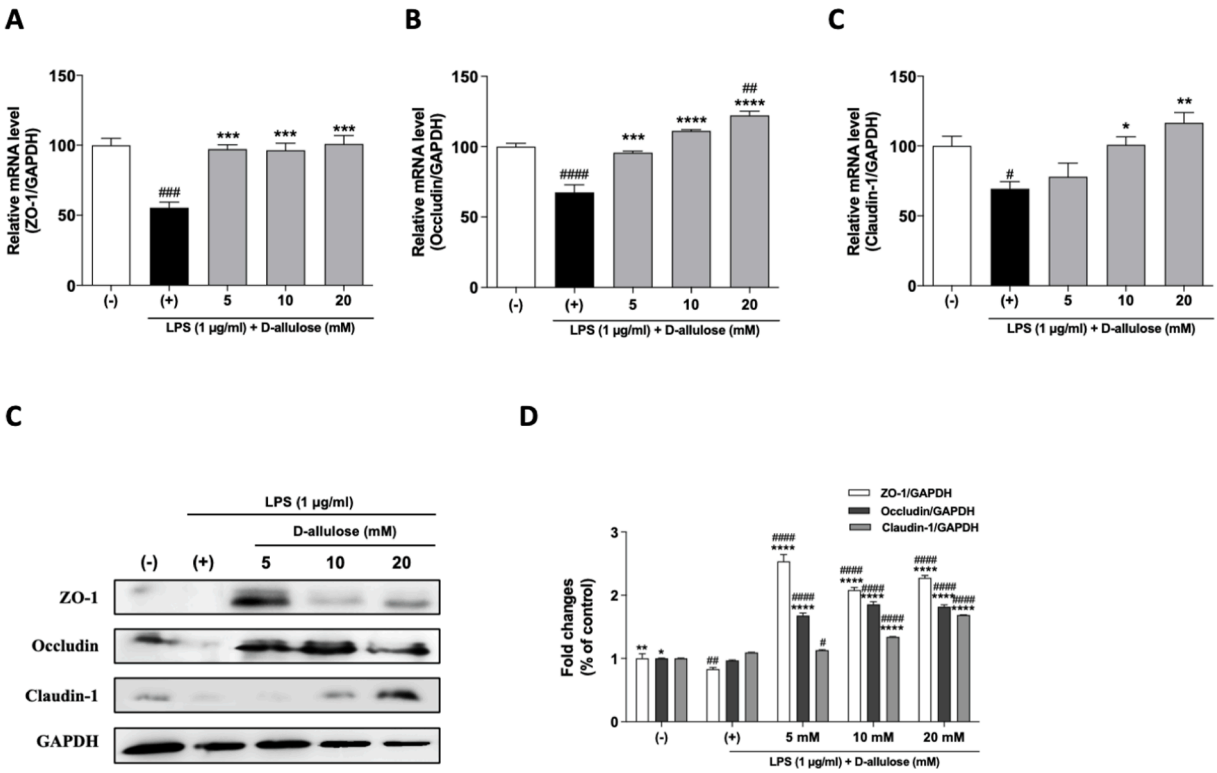

Fig. 4. Effects of D-allulose on TJ proteins and mRNA expression in LPS-induced Caco-2 cells. (A) Western blot image of ZO-1 and occludin protein expression levels. (B) Relative protein expression levels were calculated compared with the *GAPDH* housekeeping gene. The relative mRNA expression of (C) ZO-1 and (D) occludin were measured using qRT-PCR. Results are shown as mean ± standard deviation ($n = 5$). *** $P < 0.001$ and **** $P < 0.0001$ *vs.* LPS-treated group. # $P < 0.05$, ## $P < 0.005$, ### $P < 0.001$ and #### $P < 0.0001$ *vs.* control group.

and 10 mM)–treated cells showed stronger staining compared with that of the LPS-treated cells.

Claudin-1, another TJ protein, indicated co-localization with ZO-1 at the TJ, resulting in strong membrane staining throughout the control group (Fig. 6). Co-localization of claudin-1 with ZO-1 was improved in a concentration-dependent manner after D-allulose treatment.

3.6. *Effect of D-allulose on TLR4/MyD88/NF-κB signaling pathways in LPS-induced intestinal epithelial barrier dysfunction*

To investigate the regulatory mechanisms underlying the protective effects of D-allulose treatment in LPS-induced Caco-2 cells, the TLR4, MyD88, and NF-κB signaling pathways were assessed by qRT-PCR and Western blot analysis. LPS increased the expression of the TLR4 and upregulated MyD88, IRAK4, TRAF6, NF-κB p65, IKKα/β, and IKβα proteins relative to the control group (Fig. 7and Fig. S1). D-allulose treatment in the presence of LPS inhibited the activation of TLR4, MyD88, IRAK4, TRAF6, NF-κB p65, IKKα/β, and IKβα. After treatment with D-allulose, the phosphorylation of IκBα and NF-κB p65 proteins was downregulated relative to that in the LPS group ($P < 0.0001$).

4. Discussion

The intestinal barrier acts as a mechanical, biochemical, and immune defense against multiple stimuli, and it plays an important role in maintaining gut homeostasis (Fang et al., 2017). A recent study suggested that D-allulose is more effective than glucose and fructose in the enhancement of the gut barrier (Suzuki et al., 2022), but the precise mechanism by which the intestinal barrier function is enhanced through the TLR4/MyD88/NF-κB pathways has not yet been reported. In the present study, we attempted to evaluate the effects of D-allulose on intestinal inflammation and permeability. We found that D-allulose reduced intestinal permeability towards 4 kDa FITC-dextran flux, improved the expression of TJ proteins, and ameliorated LPS-induced inflammation by regulating the TLR4/MyD88/NF-κB pathway.

Intestinal epithelial barrier function is vital to gut homeostasis (Catalioto et al., 2011). Human Caco-2 cells are used to study intestinal barrier integrity *in vitro* (Hasegawa et al., 2021; He et al., 2020). Differentiated Caco-2 cells have brush borders, TJ proteins, and microvilli similar to those of human intestinal epithelial cells and show a well-established human intestinal barrier model. TNF-α and LPS have been used to induce intestinal epithelial barrier dysfunction (He et al., 2020; Li et al., 2019). They are usually used to induce intestinal barrier dysfunction models by increasing the expression levels of inflammatory factors and damaging TJs (Yang et al., 2019). Besides, the persistent inflammatory response induces functional impairment of the intestinal TJ barrier to further upregulate pro-inflammatory cytokines, including IL-1β and IL-8, constituting a vicious cycle (Lan et al., 2021). Thus, our study simulated human intestinal epithelial barrier dysfunction by inducing Caco-2 cell monolayer damage using TNF-α and LPS.

TEER and paracellular permeability are two major features used to evaluate intestinal barrier integrity (Srinivasan et al., 2015). A study investigating Caco-2 cell monolayers demonstrated that LPS could damage the intestinal barrier (Feng et al., 2022), which is consistent with our results. In our study, D-allulose significantly increased the TEER value and decreased the FITC-dextran flux compared with values associated with the LPS group. These results demonstrated that D-allulose prevented LPS-induced damage by protecting barrier integrity.

TJ proteins play an important role as a paracellular barrier of various nutrients and block bacterial translocation. Thus, they have a vital role in intestinal epithelial barrier function (Anderson & Van Itallie, 1995). TJ proteins—including ZO-1, occludin, and claudin-1—are key to TJ integrity. Moreover, these TJ proteins have roles in regulating and protecting the disruption of TJs and permeability (Al-Sadi et al., 2011;

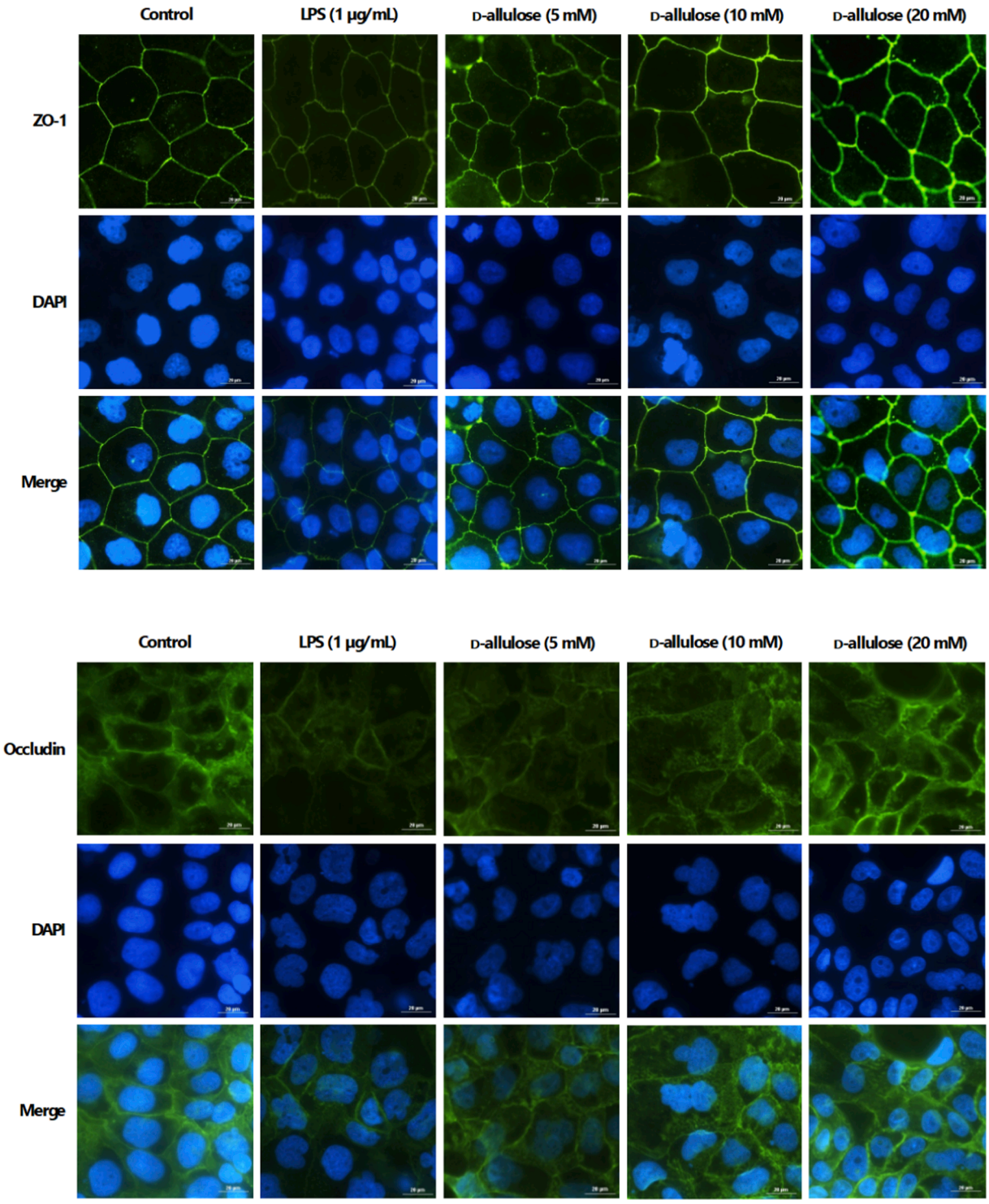

Fig. 5. Effects of D-allulose on ZO-1 and occludin localization and distribution in LPS-induced Caco-2 cells. Caco-2 monolayers were incubated with LPS (1 μg/ml) and D-allulose (5, 10, and 20 mM) for 24 h and then subjected to immunofluorescence analysis (100×).

Lee, 2015). In our study, D-allulose effectively upregulated gene and protein expression and alleviated structural damage to TJ proteins (ZO-1, occludin, and claudin-1). This was supported by another study, which showed that D-allulose potentially enhances gut mucosal barriers by upregulating TJ proteins (Suzuki et al., 2022). These results indicate that D-allulose ameliorates intestinal epithelial barrier damage by restoring the distribution structure and enhancing the expression of TJ proteins.

Inflammatory cytokines can affect the TJ conformation, which explains how inflammation can serve as a basis for altered gut function in gastrointestinal diseases (Lee, 2015; Ma, 1997). The inflammatory microenvironment affects the structure and function of intercellular junctions of epithelial cells through various mechanisms, thereby impacting the epithelial barrier and mucosal homeostasis (Luissint, Parkos, & Nusrat, 2016). IL-6 disrupts intestinal barrier function (Gong et al., 2022). TNF-α decreases the levels of claudin-1 and occludin in Caco-2 cells (Yu, Mao, Wu, Ye, & Wang, 2021). TNF-α and IL-1β induce inflammation barrier dysfunction and activation by increasing the permeability of Caco-2 monolayers (He et al., 2020). In our study, we

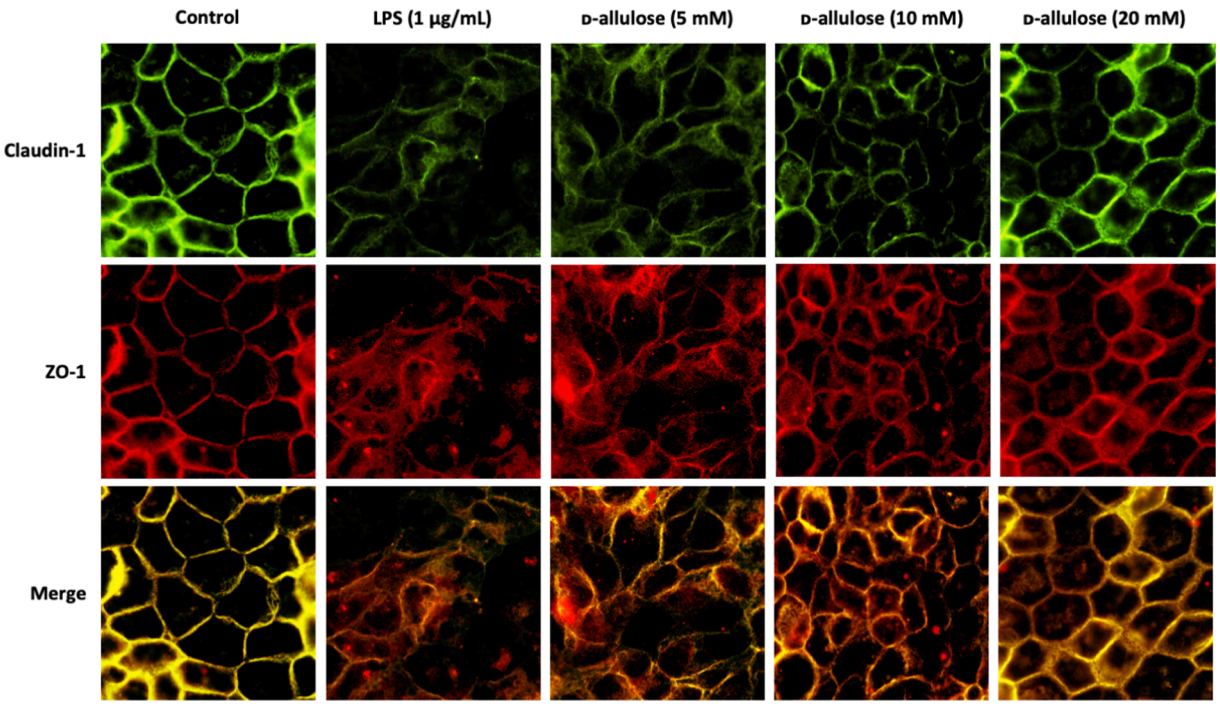

Fig. 6. Effects of D-allulose on claudin-1 with ZO-1 identification and co-localization in LPS-induced Caco-2 cells. Caco-2 monolayers were treated with LPS (1 μg/ml) and D-allulose (5, 10, and 20 mM) for 24 h and stained with both claudin-1 (green), ZO-1 (red) and co-localization (overlay). (For interpretation of the references to colour in this figure legend, the reader is referred to the web version of this article.)

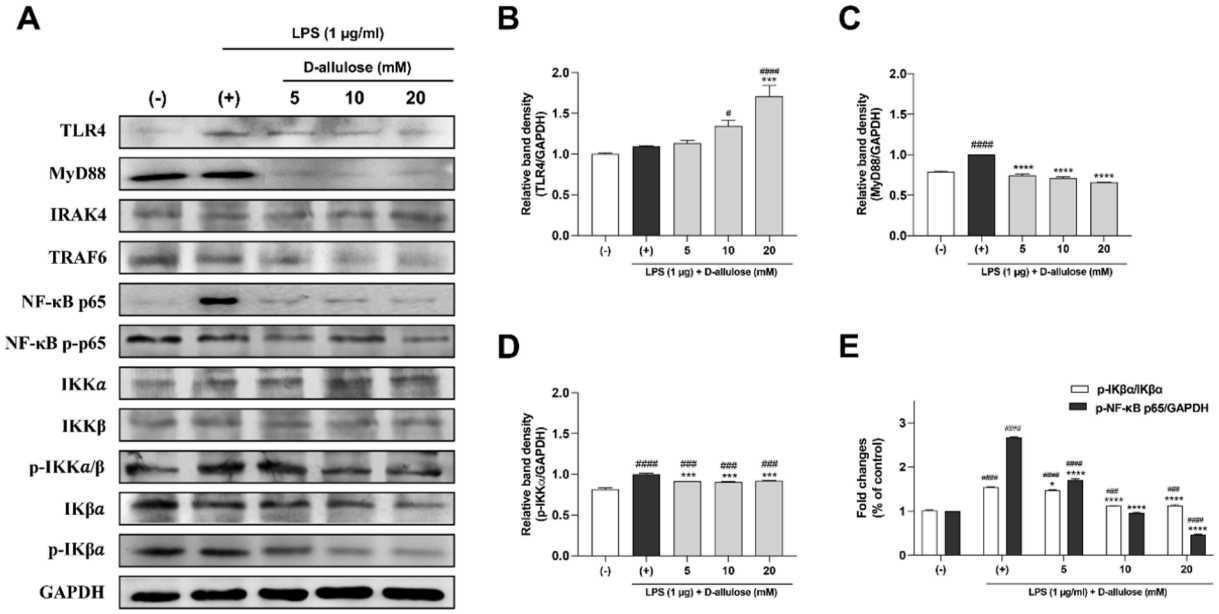

Fig. 7. Effects of D-allulose on the protein expressions of TLR4/MyD88/NF-κB in LPS-induced Caco-2 cells. NF-κB signaling protein expression were investigated by (A) Western blot analysis. The relative protein expressions of (B) MyD88/GAPDH, (C) p-IKK*α*/GAPDH, and (D) p-IKβ*α*/IKβ*α* and p-NF-κB p65/NF-κB p65 were examined. Results are shown as mean ± standard deviation (n = 5). ** $P < 0.005$, *** $P < 0.001$, and **** $P < 0.0001$ versus only LPS-treated group. ### $P < 0.001$ and #### $P < 0.0001$ versus control group.

demonstrate that LPS treatment raised the secretions of Cox-2, IL-β, IL-8, TNF-α and PGE_2 and that D-allulose treatment suppressed the production of these inflammatory cytokines in a concentration-dependent. Thus, D-allulose had a potential anti-inflammatory by inhibiting the LPS-induced production of inflammatory factors.

LPS-activated TLR4/MyD88 signaling is associated with the molecular mechanisms underlying TJ damage and inflammatory responses (Feng et al., 2022). Our results showed that D-allulose downregulated the protein expression associated with TLR4-mediated, MyD88-dependent signaling. TLR4, an immune pattern–recognition receptor, is considered a key factor in the initiation and enhancement of TLR4-mediated intestinal barrier function (Li et al., 2022). MyD88-dependent pathway–related factors, such as IRAK4, TRAF6, and IKK, are key downstream factors in the TLR4 signaling pathway and subsequent activation of the NF-kB signaling pathway (Ouyang et al., 2022). MyD88 can promote the recruitment of IRAK4 and then TRAF6, which

results in the activation of the IKK complex (Ouyang et al., 2022; Tam et al., 2021). These results suggest that D-allulose inhibited the activation of TLR4/MyD88 signaling, resulting in decreased permeability towards 4 kDa FITC-dextran. Activated MyD88 participates in the downstream activation of the NF-κB signaling pathway, leading to the activation of NF-κB (Afsharimoghaddam, Soleimani, Lashay, Dehghani, & Sepehri, 2016). Accordingly, NF-κB proteins are released and translocated into the nucleus, which play a role in regulating the expression of inflammatory genes. Here, our results show that LPS promoted the expression of phosphorylation of NF-κB p65, IKKα/β, and IκB. In contrast, D-allulose diminished the expression of these proteins, reflecting that D-allulose may alleviate intestinal epithelial function impairments by inhibiting the TLR4/MyD88/IKK/IκBα/NF-κB pathway.

5. Conclusions

This study demonstrated that D-allulose improved intestinal integrity by upregulating the TJ proteins ZO-1, occludin, and claudin-1. Additionally, D-allulose was shown to suppress the TLR4/MyD88/NF-κB signaling pathway. These beneficial effects of D-allulose may provide an important role in enhanced intestinal barrier function and suppressed inflammation and as a potential dietary supplement for functional foods or beverages to ameliorate intestinal dysfunction. Since the effects observed in cell-based experiments may not perfectly predict the outcomes in actual products, it is necessary to confirm appropriate concentrations through animal and clinical trials in the future.

Ethics statement

This work doesn't involve human or animal experiments.

CRediT authorship contribution statement

Jihye Baek: Writing – original draft, Investigation, Methodology. **Jong-Hwa Kim:** Writing – original draft, Validation. **YoHan Nam:** Methodology, Visualization. **Go-Eun Kim:** Methodology, Investigation. **Kyungheon Ryu:** Investigation, Methodology. **Soonok Sa:** Investigation, Validation. **Jung-Sook Han:** Supervision, Resources. **Wonyong Kim:** Writing – review & editing, Project administration, Conceptualization.

Declaration of Competing Interest

The authors declare that they have no known competing financial interests or personal relationships that could have appeared to influence the work reported in this paper.

Data availability

Data will be made available on request.

Acknowledgments

This work was supported by the Korea Institute of Planning and Evaluation for Technology in Food, Agriculture and Forestry (IPET), through the High Value-Added Food Technology Development Program, funded by the Ministry of Agriculture, Food and Rural Affairs (MAFRA) (322025-03) and the National Research Foundation of Korea (NRF) grant funded by the Korea government (MSIT) (NRF-2021R1C1C2003223).

Appendix A. Supplementary material

Supplementary data to this article can be found online at https://doi.org/10.1016/j.jff.2023.105721.

References

Afsharimoghaddam, A., Soleimani, M., Lashay, A., Dehghani, M., & Sepehri, Z. (2016). Controversial roles played by toll like receptor 4 in urinary bladder cancer; A systematic review. *Life Sciences, 158*, 31–36. https://doi.org/10.1016/j.lfs.2016.06.013

Al-Sadi, R., Khatib, K., Guo, S., Ye, D., Youssef, M., & Ma, T. (2011). Occludin regulates macromolecule flux across the intestinal epithelial tight junction barrier. *American Journal of Physiology. Gastrointestinal and Liver Physiology, 300*(6), G1054–G1064. https://doi.org/10.1152/ajpgi.00055.2011

Anderson, J. M., & Van Itallie, C. M. (1995). Tight junctions and the molecular basis for regulation of paracellular permeability. *The American Journal of Physiology, 269*(4 Pt 1), G467–G475. https://doi.org/10.1152/ajpgi.1995.269.4.G467

Catalioto, R. M., Maggi, C. A., & Giuliani, S. (2011). Intestinal epithelial barrier dysfunction in disease and possible therapeutical interventions. *Current Medicinal Chemistry, 18*(3), 398–426. https://doi.org/10.2174/092986711794839179

Chelakkot, C., Ghim, J., & Ryu, S. H. (2018). Mechanisms regulating intestinal barrier integrity and its pathological implications. *Experimental & Molecular Medicine, 50*(8), 1–9. https://doi.org/10.1038/s12276-018-0126-x

Chen, Y., Zhang, L., Zhang, Y., Bai, T., Song, J., Qian, W., & Hou, X. (2020). EphrinA1/EphA2 promotes epithelial hyperpermeability involving in lipopolysaccharide-induced intestinal barrier dysfunction. *Journal of Neurogastroenterology and Motility, 26*(3), 397–409. https://doi.org/10.5056/jnm19095

Chung, M. Y., Oh, D. K., & Lee, K. W. (2012). Hypoglycemic health benefits of D-psicose. *Journal of Agricultural and Food Chemistry, 60*(4), 863–869. https://doi.org/10.1021/jf204050w

Ciesielska, A., Matyjek, M., & Kwiatkowska, K. (2021). TLR4 and CD14 trafficking and its influence on LPS-induced pro-inflammatory signaling. *Cellular and Molecular Life Sciences, 78*(4), 1233–1261. https://doi.org/10.1007/s00018-020-03656-y

Dheer, R., Santaolalla, R., Davies, J. M., Lang, J. K., Phillips, M. C., Pastorini, C., … Abreu, M. T. (2016). Intestinal epithelial toll-like receptor 4 signaling affects epithelial function and colonic microbiota and promotes a risk for transmissible colitis. *Infection and Immunity, 84*(3), 798–810. https://doi.org/10.1128/IAI.01374-15

Fang, W., Bi, D., Zheng, R., Cai, N., Xu, H., Zhou, R., … Xu, X. (2017). Identification and activation of TLR4-mediated signalling pathways by alginate-derived guluronate oligosaccharide in RAW264.7 macrophages. *Scientific Reports, 7*(1), 1663. https://doi.org/10.1038/s41598-017-01868-0

FDA. (2012). GRAS Notice Inventory: No. GRN 000400. D–Psicose, CJ CheilJedang. United States: Food and Drug Administration (FDA).

Feng, R., Adeniran, S. O., Huang, F., Li, Y., Ma, M., Zheng, P., & Zhang, G. (2022). The ameliorative effect of melatonin on LPS-induced Sertoli cells inflammatory and tight junctions damage via suppression of the TLR4/MyD88/NF-kappaB signaling pathway in newborn calf. *Theriogenology, 179*, 103–116. https://doi.org/10.1016/j.theriogenology.2021.11.020

Franchi, F., Yaranov, D. M., Rollini, F., Rivas, A., Rivas Rios, J., Been, L., … Mooradian, A. D. (2021). Effects of D-allulose on glucose tolerance and insulin response to a standard oral sucrose load: Results of a prospective, randomized, crossover study. *BMJ Open Diabetes Research & Care, 9*(1), Article e001939. https://doi.org/10.1136/bmjdrc-2020-001939

Gong, S., Zheng, J., Zhang, J., Wang, Y., Xie, Z., Wang, Y., & Han, J. (2022). Taxifolin ameliorates lipopolysaccharide-induced intestinal epithelial barrier dysfunction via attenuating NF-kappa B/MLCK pathway in a Caco-2 cell monolayer model. *Food Research International, 158*, Article 111502. https://doi.org/10.1016/j.foodres.2022.111502

Gou, Y., Liu, B., Cheng, M., Yamada, T., Iida, T., Wang, S., … Koike, T. (2021). D-allulose ameliorates skeletal muscle insulin resistance in high-fat diet-fed rats. *Molecules, 26*(20), Article 6310. https://doi.org/10.3390/molecules26206310

Hasegawa, T., Mizugaki, A., Inoue, Y., Kato, H., & Murakami, H. (2021). Cystine reduces tight junction permeability and intestinal inflammation induced by oxidative stress in Caco-2 cells. *Amino Acids, 53*(7), 1021–1032. https://doi.org/10.1007/s00726-021-03001-y

Hayashi, N., Iida, T., Yamada, T., Okuma, K., Takehara, I., Yamamoto, T., … Tokuda, M. (2010). Study on the postprandial blood glucose suppression effect of D-psicose in borderline diabetes and the safety of long-term ingestion by normal human subjects. *Bioscience, Biotechnology, and Biochemistry, 74*(3), 510–519. https://doi.org/10.1271/bbb.90707

He, C., Deng, J., Hu, X., Zhou, S., Wu, J., Xiao, D., … Yang, X. (2019). Vitamin A inhibits the action of LPS on the intestinal epithelial barrier function and tight junction proteins. *Food & Function, 10*(2), 1235–1242. https://doi.org/10.1039/c8fo01123k

He, S., Guo, Y., Zhao, J., Xu, X., Wang, N., & Liu, Q. (2020). Ferulic acid ameliorates lipopolysaccharide-induced barrier dysfunction via microRNA-200c-3p-mediated activation of PI3K/AKT pathway in Caco-2 cells. *Frontiers in Pharmacology, 11*, Article 376. https://doi.org/10.3389/fphar.2020.00376

Hossain, A., Yamaguchi, F., Matsuo, T., Tsukamoto, I., Toyoda, Y., Ogawa, M., … Tokuda, M. (2015). Rare sugar D-allulose: Potential role and therapeutic monitoring in maintaining obesity and type 2 diabetes mellitus. *Pharmacology & Therapeutics, 155*, 49–59. https://doi.org/10.1016/j.pharmthera.2015.08.004

Kawai, T., & Akira, S. (2006). TLR signaling. *Cell Death and Differentiation, 13*(5), 816–825. https://doi.org/10.1038/sj.cdd.4401850

Lan, H., Zhang, L.-Y., He, W., Li, W.-Y., Zeng, Z., Qian, B., … Song, J.-L. (2021). Sinapic acid alleviated inflammation-induced intestinal epithelial barrier dysfunction in lipopolysaccharide-(LPS-) treated caco-2 cells. *Mediators of Inflammation, 2021*.

Lee, S. H. (2015). Intestinal permeability regulation by tight junction: Implication on inflammatory bowel diseases. *Intestinal Research, 13*(1), 11–18. https://doi.org/10.5217/ir.2015.13.1.11

Lee, G.-H., Peng, C., Lee, H.-Y., Park, S.-A., Hoang, T.-H., Kim, J. H., … Chae, H.-J. (2021). D-allulose ameliorates adiposity through the AMPK-SIRT1-PGC-1α pathway in HFD-induced SD rats. *Food & Nutrition Research, 65*.

Li, J., Jia, Q., Liu, Y., Chen, D., Fang, Z., Liu, Y., … Chen, H. (2022). Different structures of arabinoxylan hydrolysates alleviated Caco-2 cell barrier damage by regulating the TLRs/MyD88/NF-kappaB pathway. *Foods, 11*(21). https://doi.org/10.3390/foods11213535

Li, Y., Tian, X., Li, S., Chang, L., Sun, P., Lu, Y., … Kang, W. (2019). Total polysaccharides of adlay bran (*Coix lachryma-jobi* L.) improve TNF-alpha induced epithelial barrier dysfunction in Caco-2 cells via inhibition of the inflammatory response. *Food & Function, 10*(5), 2906–2913. https://doi.org/10.1039/c9fo00590k

Luissint, A. C., Parkos, C. A., & Nusrat, A. (2016). Inflammation and the intestinal barrier: Leukocyte-epithelial cell interactions, cell junction remodeling, and mucosal repair. *Gastroenterology, 151*(4), 616–632. https://doi.org/10.1053/j.gastro.2016.07.008

Luo, H., Guo, P., & Zhou, Q. (2012). Role of TLR4/NF-kappaB in damage to intestinal mucosa barrier function and bacterial translocation in rats exposed to hypoxia. *PLoS ONE, 7*(10), Article e46291. https://doi.org/10.1371/journal.pone.0046291

Ma, T. Y. (1997). Intestinal epithelial barrier dysfunction in Crohn's disease. *Proceedings of the Society for Experimental Biology and Medicine, 214*(4), 318–327. https://doi.org/10.3181/00379727-214-44099

Matsuo, T., Suzuki, H., Hashiguchi, M., & Izumori, K. (2002). D-psicose is a rare sugar that provides no energy to growing rats. *Journal of Nutritional Science and Vitaminology (Tokyo), 48*(1), 77–80. https://doi.org/10.3177/jnsv.48.77

Niibo, M., Kanasaki, A., Iida, T., Ohnishi, K., Ozaki, T., Akimitsu, K., & Minamino, T. (2022). D-allulose protects against diabetic nephropathy progression in otsuka long-evans tokushima fatty rats with type 2 diabetes. *PLoS ONE, 17*(1), Article e0263300. https://doi.org/10.1371/journal.pone.0263300

Ouyang, F., Li, B., Wang, Y., Xu, L., Li, D., Li, F., & Sun-Waterhouse, D. (2022). Attenuation of palmitic acid-induced intestinal epithelial barrier dysfunction by 6-shogaol in Caco-2 cells: The role of miR-216a-5p/TLR4/NF-kappaB axis. *Metabolites, 12*(11), Article 1028. https://doi.org/10.3390/metabo12111028

Srinivasan, B., Kolli, A. R., Esch, M. B., Abaci, H. E., Shuler, M. L., & Hickman, J. J. (2015). TEER measurement techniques for in vitro barrier model systems. *Journal of Laboratory Automation, 20*(2), 107–126. https://doi.org/10.1177/2211068214561025

Suzuki, T., Sato, Y., Kadoya, S., Takahashi, T., Otomo, M., Kobayashi, H., … Ferraris, R. P. (2022). Comparative effects of allulose, fructose, and glucose on the small intestine. *Nutrients, 14*(15), Article 3230. https://doi.org/10.3390/nu14153230

Tam, J. S. Y., Coller, J. K., Hughes, P. A., Prestidge, C. A., & Bowen, J. M. (2021). Toll-like receptor 4 (TLR4) antagonists as potential therapeutics for intestinal inflammation. *Indian Journal of Gastroenterology, 40*(1), 5–21. https://doi.org/10.1007/s12664-020-01114-y

Wolfe, K. L., & Liu, R. H. (2007). Cellular antioxidant activity (CAA) assay for assessing antioxidants, foods, and dietary supplements. *Journal of Agricultural and Food Chemistry, 55*(22), 8896–8907. https://doi.org/10.1021/jf0715166

Yang, H. S., Haj, F. G., Lee, M., Kang, I., Zhang, G., & Lee, Y. (2019). Laminaria japonica extract enhances intestinal barrier function by altering inflammatory response and tight junction-related protein in lipopolysaccharide-stimulated Caco-2 cells. *Nutrients, 11*(5). https://doi.org/10.3390/nu11051001

Yu, L. M., Mao, L. Q., Wu, C. Y., Ye, W., & Wang, X. (2021). Chlorogenic acid improves intestinal barrier function by downregulating CD14 to inhibit the NF-κB signaling pathway. *Journal of Functional Foods, 85*, Article 104640.